J. exp. Biol. 157, 183–204 (1991)
Printed in Great Britain © The Company of Biologists Limited 1991

VERTICAL FLIGHT IN THE GREATER HORSESHOE BAT *RHINOLOPHUS FERRUMEQUINUM*

BY H. D. J. N. ALDRIDGE*

Department of Zoology, University of Bristol, Woodland Road, Bristol BS8 1UG

Accepted 4 December 1990

Summary

The kinematics, aerodynamics and energetics of vertical flight in *Rhinolophus ferrumequinum* (Schreber) are described. During the downstroke the resultant force generated by the wings tends to accelerate the animal upwards and forwards. Towards the end of the downstroke the wings generate negative thrust and, consequently, the animal accelerates backwards. When, during the upstroke, the wings are accelerated backwards (the 'flick') a significant thrust is generated. Total specific mechanical power is approximately $11.92\,W\,kg^{-1}$, of which 84% is required during the downstroke.

Introduction

Hovering can be defined as flight in which no net thrust is generated. Normally animals use it to remain stationary in the air as they sip nectar or glean resting prey. It can, however, be used to make vertical manoeuvres; i.e. although there is no net horizontal force the net vertical force is greater than the animal's weight, thus tending to accelerate the animal vertically upwards. This behaviour has been observed in a number of bat species, such as the common slit-faced bat *Nycteris thebaica*, which roosts in hollow trees, the internal diameters of which are often no greater than the bats' wing spans. When returning to roost, the animals are forced to 'hover' vertically up these trees (Aldridge *et al.* 1990). Similarly, *Rhinolophus ferrumequinum* sometimes roosts in narrow and derelict chimneys and has been observed hovering up these structures (R. E. Stebbings, personal communication).

When hovering and flying slowly, many vertebrates use a 'tip-reversal' upstroke, in which the 'arm' wings (the portion of the wings between the wrist and the shoulder; the pro- and plagiopatagia in bats, the secondary feathers in birds) are highly flexed and aerodynamically inactive, but the 'hand' wings (the chiropata-

* Present address: Agricultural and Food Research Council, Wiltshire Court, Farnsby Street, Swindon, Wiltshire SN1 5ET, UK.

Key words: bat, vertical flight, kinematics, aerodynamics, energetics, *Rhinolophus ferrumequinum*.

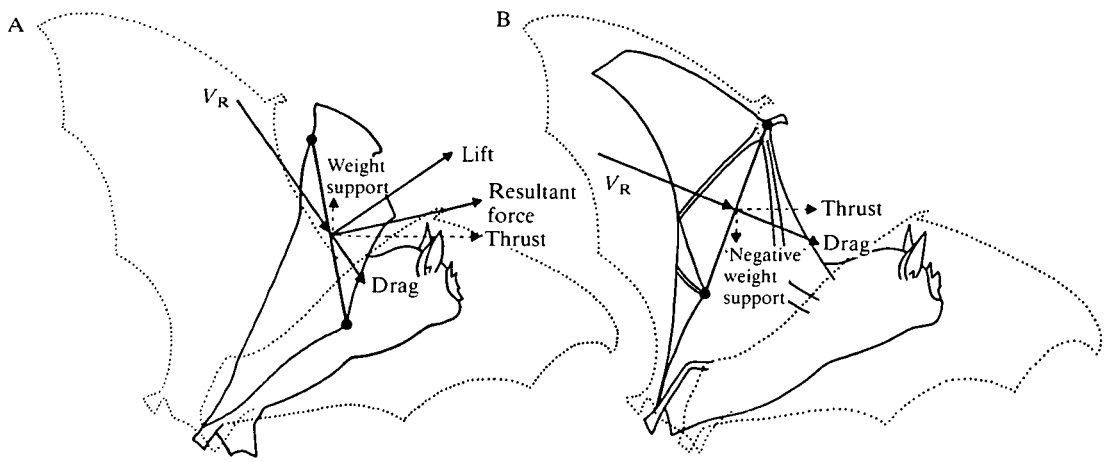

Fig. 1. Possible mechanisms of lift generation during the 'tip-reversal' upstroke. (A) The wing is accelerated backwards and upwards and the relative airflow strikes its morphologically dorsal surface; thrust and weight support are generated. (B) During the flick, the relative airflow strikes the wing's dorsal surface at an angle significantly higher than the steady-state stall angle; consequently thrust is generated. V_R is the resultant velocity of the wing.

gia in bats, the primary feathers in birds) are fully extended and moved backwards and upwards (relative to the animal's centre of mass), with their ventral surfaces facing upwards and forwards (Eisentraut, 1936; Brown, 1948; Norberg, 1970, 1976*a*,*b*; Altenbach, 1979; Aldridge, 1986, 1987*a*; von Helversen, 1986).

Some authors (e.g. Norberg, 1970, 1976*a*,*b*; von Helversen, 1986; Aldridge, 1987*a*) are agreed that this movement produces thrust during slow forward flight. Two mechanisms of upstroke thrust generation have been suggested. First, thrust is generated because the *incidence* angles of the chiropatagia are higher than the *zero-lift* angle but lower than the *steady-state stall* angle (Fig. 1A). Second, because at the end of the upstroke the wings are accelerated backwards (the 'flick'), a large drag force is generated. This force is directed forwards and acts as thrust (Fig. 1B; Eisentraut, 1936; Norberg, 1976*a*; Altenbach, 1979; Aldridge, 1987*a*). Similar mechanisms might also operate during the hovering upstroke, although Norberg (1976*b*) did not find significant upstroke thrust in a hovering brown long-eared bat, *Plecotus auritus*, and concluded that the upstroke was mainly a recovery stroke.

It has proved difficult to verify, experimentally, that during the 'tip-reversal' upstroke the wings generate weight support or thrust. For example Rayner *et al.* (1986) were unable to visualise upstroke circulations in the wake of slow-flying bats, although they did acknowledge that these might have been eliminated by the much larger air movements produced during the downstroke. In a previous study, I measured horizontal accelerations during the wingbeat in a number of bats belonging to six species (Aldridge, 1987*a*). I found that the bat's forward velocities tended to increase during or immediately after the 'tip-reversal' upstroke whe

their wings were accelerated upwards and backwards (relative to the animal), indicating that thrust was being generated.

I showed in that paper that the accelerations and decelerations during a wingbeat could be used as independent measures of upstroke function. This should also be feasible for hovering animals. In hovering, the vertical force generated by the wings during the downstroke is opposite in direction, but equal in magnitude, to the animal's weight. Therefore, hovering animals do not accelerate vertically during the downstroke. If the wings do not generate any significant forces during the upstroke, we can predict that, owing to the force of gravity, the animal should decelerate and, eventually, start to accelerate downwards at about $9.81\,m\,s^{-2}$. Consequently, each hovering wingbeat should be characterized by vertical accelerations and decelerations.

I found that captive *R. ferrumequinum* would not hover willingly, and would do so only for very short periods. The bats would, however, 'hover' vertically up a narrow flight tunnel, thus offering me the opportunity to study the kinematics and aerodynamics of this flight behaviour. Indeed vertical flight has certain advantages over hovering flight, because the hovering wingbeats are separated spatially and are therefore amenable to analysis using a multi-flash photographic technique (e.g. Rayner and Aldridge, 1985).

The primary aim of this study was to establish whether the wings are active during the 'tip-reversal' upstroke. I was also interested in estimating the power required by *R. ferrumequinum* for this expensive flight behaviour.

Materials and methods

The individual *R. ferrumequinum* used in this study was the same as that used in my previous studies (Aldridge, 1986, 1987*a*,*b*). Descriptions of husbandry and training can be found in those papers and details of the bat's morphology are given in Table 1.

Photography

The bat was photographed as it flew vertically through a 2 m high plywood flight tunnel (width 0.4 m, breadth 0.4 m). The working section was situated midway

Table 1. *Morphological parameters of the individual* Rhinolophus ferrumequinum *used in these experiments*

Mass, M (kg)	0.0222
Span, b (m)	0.36
Area, S (m^2)	0.0222
Wing loading, Q_s ($N\,m^{-2}$)	9.8
Aspect ratio, R	5.8
Equivalent flat plate area, A_e (m^2)	1.62×10^{-3}
Wing moment of inertia, I ($kg.m^2$)	
Fully extended (downstroke)	7.23×10^{-6}
Flexed (upstroke)	2.49×10^{-6}

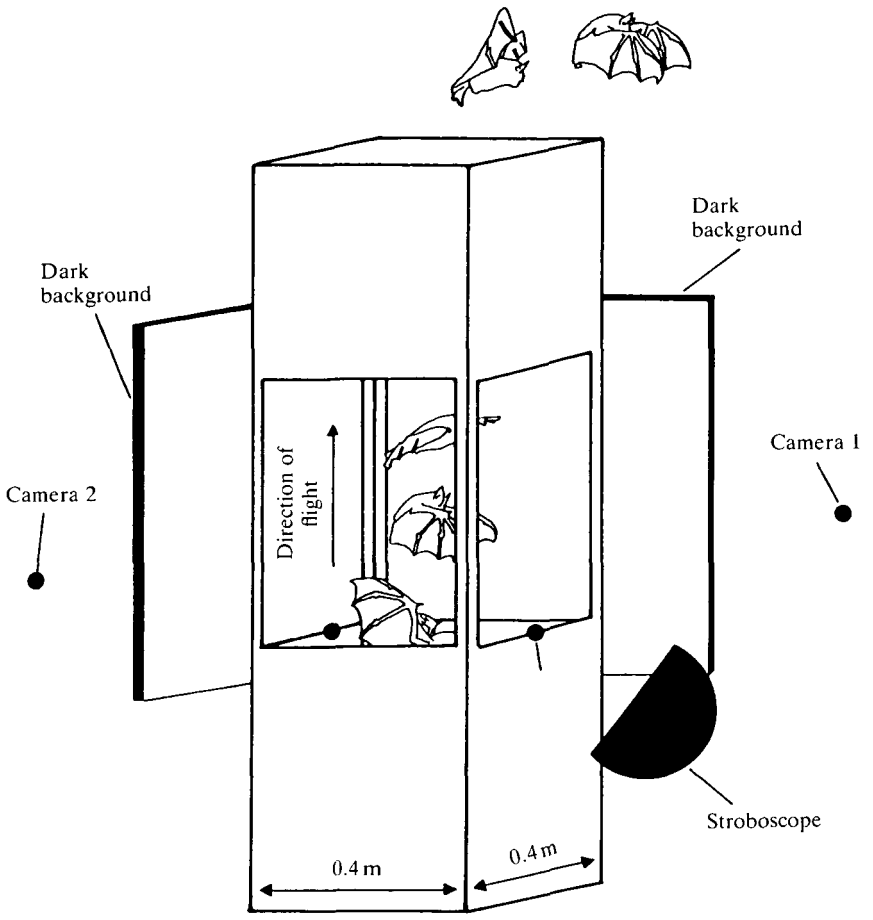

Fig. 2. The experimental configuration. The bat flies vertically upwards through the flight tunnel. A dark-activated switch opens the camera shutters for approximately 1 s, and the bat is lit – against black backgrounds – by a stroboscope.

along the tunnel and consisted of four 0.5 m sheets of 3 mm Perspex (Fig. 2), which could be removed between experiments. By the time the experiments described here were performed, the bat was hand-tame and would respond to an auditory signal by landing on a perch or on my hand. Once held, the bat could be placed upon a perch situated at the bottom of the flight tunnel. Normally it would remain on the perch until I clicked my fingers, when it would fly up the tunnel and land on another perch, to be rewarded with a small piece of a mealworm (*Tenebrio molitor*).

As it flew up the tunnel the bat interrupted an infrared beam, activating a dark-sensitive switch and triggering the two Nikon SLR FM and FM2 cameras (fitted with Nikkor 55 mm f2.8 and f3.5 lenses, respectively). The cameras were arranged on mutually perpendicular axes with their film-planes parallel to the sides of the

flight tunnel (Fig. 2). As it flew up the tunnel the bat was illuminated by a stroboscope (Dawe Instruments 1203C 'Strobosun') flashing at 100 Hz.

Before each series of experimental flights I took photographs of a 0.15 m reference cube which was suspended within the tunnel. For each flight two photographs were taken showing multiple images of the bat from the front and the side. Of these two photographs only the lateral view was analyzed. The frontal view was used to check that the bat had flown up the centre of the tunnel.

Analysis

The data were transcribed by projecting the images onto paper on which the positions of the nose-leaf, the base of the tail, the wrist and the wingtip were marked. Positional data were used to calculate wing positive elevation, θ_u, wing negative elevation, θ_d, wingbeat amplitude (twice the angular excursion of one wing), θ, and wrist strokeplane angle, β, which is defined as the angle between the horizontal and a line drawn between the position of the wrist at the beginning and end of the downstroke (Fig. 3). Wingbeat frequency, n, was also recorded for each flight. The angle of the bat to the horizontal (body angle, α) was calculated as

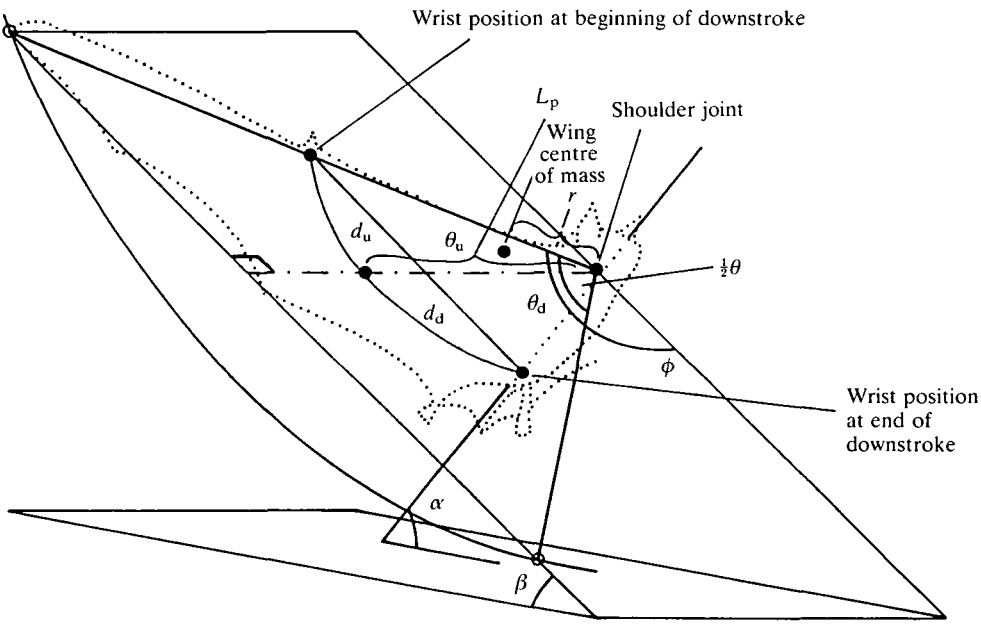

Fig. 3. Diagram showing the various terms used in the text. β is the strokeplane angle, $\theta/2$ is the wing's angular excursion and θ_u and θ_d are the wing's positive and negative elevations, respectively. ϕ is the positional angle and α is body angle. d_u and d_d are the distances, within the strokeplane, between the wrist and the longitudinal axis of the body at the beginning and end of the downstroke, respectively. l_p is the distance between a point midway between the two humeral joints and the wrist when the wing is fully extended and r is the distance between the centres of mass of the body and wing.

being the angle made with the horizontal by a line drawn between the nose-leaf and the base of the tail (Fig. 3).

Image coordinates were converted into estimates of actual distances using magnification factors calculated using the dimensions of the photographic images of the 0.15 m cube. For each data point, I calculated the bat's vertical and horizontal accelerations (a_z and a_x, respectively) using Lanczos' (1957) method, as described in Rayner and Aldridge (1985).

The wings' positive and negative elevations were estimated using the equations:

$$d_u/l_p = \tan\theta_u \quad (1)$$

and

$$d_d/l_p = \tan\theta_d, \quad (2)$$

where d_u and d_d are the distances, within the strokeplane, between the wrist and the longitudinal axis of the body at the beginning and end of the downstroke, respectively. l_p is the distance between a point midway between the two humeral joints and the wrist when the wing is fully extended. θ is twice the sum of θ_u and θ_d.

Errors

As described in Aldridge (1988), there are two important sources of positional error in this technique: parallax errors and errors due to the fact that at any instant the precise distance between the camera and the bat is unknown. Maximum parallax error will occur at the edges of the frame and I estimated it to be approximately 10 % (with a bat-to-camera distance of about 1 m; Aldridge, 1988). Towards the middle of the frame, parallax error will be negligible, and for this reason I only analyzed those images that fell within the central two-thirds of the frame. I estimated that the maximum error due to variation in the distance of the bat from the camera was 4 % (Aldridge, 1988). Errors in θ_u, θ_d and θ are likely to be greater than those in position, because it is difficult to determine accurately the beginning and end of the downstroke.

Forces

During a wingbeat an animal flying vertically experiences six forces; its weight, Mg (where M is body mass and g is the acceleration due to gravity); induced drag, D_i; parasite drag, D_{par}; profile drag, D_{pro}; inertial forces, F_b; and lift, L (Fig. 4). During the downstroke the wings move forwards and downwards generating L, F_b, D_i and D_{pro}, the consequent upward movement of the body generating D_{par}. Of these forces L, D_i and F_b will tend to accelerate the animal upwards, while Mg, D_{pro} and D_{par} will retard its upward movement. Similarly, F_b, D_i and D_{pro} will tend to accelerate the animal backwards, although L should counteract this. During the upstroke, F_b, D_i and D_{pro} will tend to accelerate the animal downwards and forwards. If lift is generated during the upstroke then it is likely to be directed

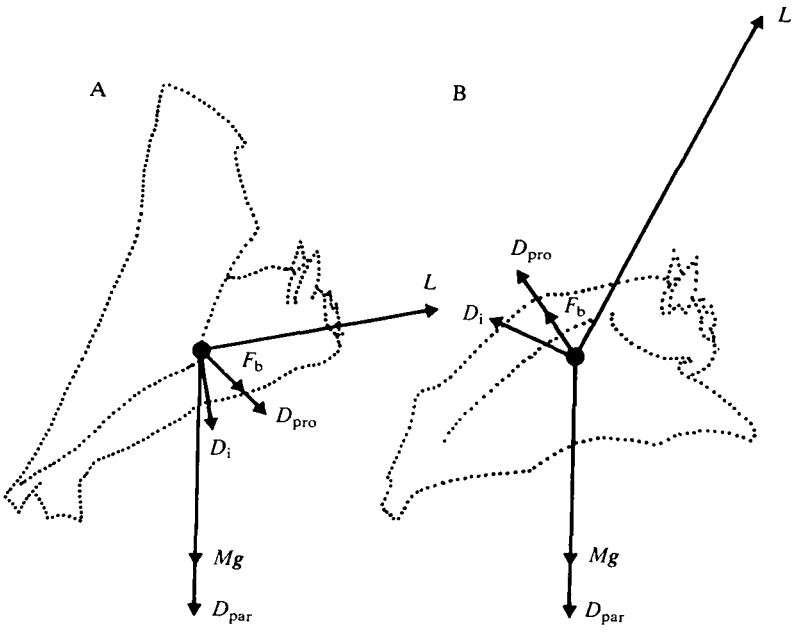

Fig. 4. Mean forces acting on a bat flying vertically. (A) Upstroke; (B) downstroke. Mg is body weight (where M is body mass and g is the acceleration due to gravity), D_i is induced drag, D_{par} is parasite drag, D_{pro} is profile drag, F_b is inertial force and L is lift.

forwards. The instantaneous vertical, $F_{vert}(t)$, and horizontal, $F_{hor}(t)$, forces acting on the bat are, therefore:

$$F_{vert}(t) = L_{vert}(t) + F_{b,vert}(t) + D_{pro,vert}(t) + D_{i,vert}(t) - D_{par,vert}(t) - Mg \quad (3)$$

and

$$F_{hor}(t) = L_{hor}(t) - F_{b,hor}(t) - D_{i,hor}(t) - D_{pro,hor}(t) - D_{par,hor}(t)\,, \quad (4)$$

during the downstroke, and:

$$F_{vert}(t) = L_{vert}(t) - F_{b,vert}(t) - D_{i,vert}(t) - D_{pro,vert}(t) - D_{par,vert}(t) - Mg \quad (5)$$

and

$$F_{hor}(t) = L_{hor}(t) + F_{b,hor}(t) + D_{i,hor}(t) + D_{pro,hor}(t) - D_{par,hor}(t) \quad (6)$$

during the upstroke. Where $L_{vert}(t)$, $L_{hor}(t)$, $F_{b,vert}(t)$, $F_{b,hor}(t)$, $D_{i,vert}(t)$, $D_{i,hor}(t)$, $D_{pro,vert}(t)$, $D_{pro,hor}(t)$, $D_{par,vert}(t)$ and $D_{par,hor}(t)$ are, respectively, the instantaneous vertical and horizontal components of L, F_b, D_i, D_{pro} and D_{par}.

$F_b(t)$, the instantaneous inertial force acting on the animal, can be calculated using the method outlined in Aldridge (1987*a*). The angular velocity of a wing is:

$$\omega = d\phi/dt\,, \quad (7)$$

where ϕ is the positional angle (Fig. 3). Wing angular acceleration is, therefore:

$$\dot{\omega} = \mathrm{d}^2\phi/\mathrm{d}t^2, \tag{8}$$

and the acceleration of the wing centre of mass is:

$$a_w(t) = r\dot{\omega}, \tag{9}$$

where r is the distance between the centres of mass of the body and wing (Fig. 3).

Unfortunately, soon after the experiments described here were performed the bat died of an undiagnosed infection. When it was dead I removed its right wing at the shoulder joint (the right leg and the right side of the uropatagium were not included) and, after fully extending it, I attached it to a small card. I suspended the card plus wing sequentially from three points, thus locating its centre of mass. I knew the position of the centre of mass of the card and was therefore able to estimate r.

The total inertial force acting on the body due to the acceleration of one wing is:

$$F_w(t) = M_w a_w(t), \tag{10}$$

where M_w is the mass of the wing. In the absence of actual measurements of wing mass, Aldridge's (1987*a*) equation can be used:

$$M_w = 5.77S^{2.12}, \tag{11}$$

where S is total wing area (note: this equation was given incorrectly as $M_w=0.761S^{2.12}$ in Aldridge, 1987*a*).

The vertical component of $F_w(t)$ is:

$$F_{w,vert}(t) = F_w(t)\sin\beta. \tag{12}$$

The total vertical force, due to wing oscillation, experienced by the bat is therefore:

$$F_{b,vert}(t) = 2[F_w(t)\sin\beta], \tag{13}$$

and, finally, the vertical acceleration experienced by the animal due to wing acceleration is:

$$a_{b,vert}(t) = 2[F_w(t)\sin\beta]/M. \tag{14}$$

Similarly, the instantaneous horizontal acceleration, $a_{b,hor}(t)$, experienced by the animal due to wing acceleration is:

$$a_{b,hor}(t) = 2[F_w(t)\cos\beta]/M. \tag{15}$$

The acceleration and deceleration of the wings during a wingbeat will, inevitably, set the air surrounding the wings into motion. As a result, there is an apparent increase in wing mass; *wing virtual mass*, or added mass, m_v (Ellington, 1984). Theoretically, this mass is equal to the mass of air in an imaginary cylinder around the wing with the wing chord as its diameter. The virtual mass of a wing element at a distance l from the humeral joint can be calculated as:

$$m_v' = \rho\pi c^2/4, \tag{16}$$

where c is wing chord length and ρ is air density. The total virtual mass of a wing is:

$$m_v = (\rho\pi/4) \int_{l=0}^{l=l_w} c^2 . dl , \tag{17}$$

where l_w is wing length (Ellington, 1984).

In calculating the inertial forces acting on the bat, I assumed that the wings were either accelerating or decelerating throughout the wingbeat and thus included m_v as a constant. This probably overestimates the apparent mass of the wings, but I do not believe this to be significant.

$D_{par}(t)$ is the sum of the instantaneous pressure and friction drags of the body and will tend to oppose the animal's vertical movement. $D_{par}(t)$ can be calculated as:

$$D_{par}(t) = (1/2)\rho V(t)^2 S_b C_{D,par} , \tag{18}$$

where S_b is the projected area of the body perpendicular to the airflow and $C_{D,par}$ is the parasite drag coefficient.

$S_b C_{D,par}$ can be replaced by A_e, which is the area of a flat plate with a parasite drag coefficient equal to 1, which gives the same drag as the body. Pennycuick (1975) developed an equation by which A_e for an untilted body can be calculated, assuming a drag coefficient of 0.43. Pennycuick *et al.* (1988), however, recommend a $C_{D,par}$ value of 0.40.

In this study, the bat moved vertically with its dorsal surface meeting the downward airflow. I calculated A_e as being:

$$A_e = 0.40(S_{b,hor}\cos\alpha) , \tag{19}$$

where $S_{b,hor}$ is the projected area of the body on the horizontal plane.

$D_{pro}(t)$ is the sum of the instantaneous pressure and friction drags of the wings and can be calculated as:

$$D_{pro}(t) = (1/2)\rho V_R(t)^2 S C_{D,pro} , \tag{20}$$

where $V_R(t)$ is the resultant velocity of the wing and $C_{D,pro}$ is the profile drag coefficient, to which, following Rayner (1979), I have given a value of 0.02. V_R for a whole wing can be estimated as being the resultant velocity of a point 0.7 times wing length from the humeral joint. This is the point at which the lift generated by a flapping wing can be considered to act (Pennycuick, 1967).

The instantaneous resultant velocity of a wing point, $V_R(t)$, is the resultant of flapping velocity, $V_f(t)$, induced velocity, $V_i(t)$ and the bat's resultant velocity, V. $V_f(t)$, for a point 0.7 times wing length from the humeral joint is:

$$V_f(t) = 0.7 l_w \omega . \tag{21}$$

$V_R(t)$ for this point is therefore:

$$V_R(t)^2 = [V_i(t) + V(t)]^2 + V_f(t)^2 - 2[V_i(t) + V(t)]V_f(t)\cos(90 - \beta) \tag{22}$$

during the downstroke and:

$$V_R(t)^2 = [V_i(t) + V(t)]^2 + V_f(t)^2 - 2[V_i(t) + V(t)]V_f(t)\cos(90 + \beta) \quad (23)$$

during the upstroke (with wings flexed).

Power requirements

The total mechanical power required by a hovering animal can be calculated as:

$$P_a = \int_{t=0}^{t=T} [P_i(t) + P_{par}(t) + P_{pro}(t) + P_{iner}(t)]dt, \quad (24)$$

where $P_i(t)$, $P_{par}(t)$, $P_{pro}(t)$ and $P_{iner}(t)$ are the instantaneous values of induced, parasite, profile, inertial power, respectively, and T is the duration of the wingbeat (i.e. $T=1/n$). If the upstroke is active in lift generation, then power should be calculated separately for the upstroke and downstroke. Thus, equation 24 becomes:

$$P_a = \int_{t=0}^{t=T/2} [P_a(t)]dt + \int_{t=T/2}^{t=T} [P_a(t)]dt, \quad (25)$$

where $P_a(t)$ is the sum of the instantaneous values of the four power components.

A minimum value of $P_i(t)$ can be calculated using the Rankine–Froude momentum jet theory, as applied to flapping flight by Pennycuick (1975). In hovering flight the bat flaps its wings, sweeping out a wing disk, which has a disk area S_d. The movement of the wings causes the air to accelerate downwards and to reach an induced velocity, V_i, as it passes through the disk. The power required to maintain this flow, $P_i(t)$, is the product of lift L and V_i:

$$P_i(t) = LV_i = L^2/2\rho V^2 S_d, \quad (26)$$

where S_d is defined as:

$$S_d = \pi b^2/4, \quad (27)$$

where b is wing span. I calculated L as being the resultant of $L_{vert}(t)$ and $L_{hor}(t)$, which I estimated as:

$$L_{vert}(t) = Ma_z(t) + Mg + D_{par}(t) - F_{b,vert}(t) \quad (28)$$

and

$$L_{hor}(t) = Ma_x(t) + F_b(t) \quad (29)$$

during the downstroke and

$$L_{vert}(t) = Ma_z(t) + Mg + D_{par}(t) + F_b(t) \quad (30)$$

and

$$L_{hor}(t) = Ma_x(t) - F_b(t) \quad (31)$$

during the upstroke.

Equation 26 will give a minimum value for induced power, because it assumes that the air passes through all sectors of the disk at exactly the same value of V_i, and that the air outside the disk remains unaccelerated. In reality, the speed of the air as it passes the wing will vary and there will be no clear distinction between the

air flowing through the disk and still air outside it. Therefore, the animal does more work to generate the momentum needed to support its weight than indicated by equation 26 and this deviation from the ideal is represented by the *induced power factor*, k. Total mechanical power is therefore:

$$P_a = k\left[\int_{t=0}^{t=T} P_i(t)\right]dt + \left[\int_{t=0}^{t=T} P_{par}(t) + P_{pro}(t) + P_{iner}(t)\right]dt. \quad (32)$$

Tucker (1973) gave k a value of 1.43, while Pennycuick (1975) suggested that k could be set at 1.2 if no other value was available. In these calculations I assumed a value of 1.2. $P_{par}(t)$ is the power required to overcome the drag of the body, $D_{par}(t)$. In equation 18 I have defined $D_{par}(t)$ and it can be shown that $P_{par}(t)$ is:

$$P_{par}(t) = D_{par}(t)V(t). \quad (33)$$

P_{iner} is the power required to accelerate and decelerate the wings and is thought to be important in hovering flight (Pennycuick, 1975). It is calculated as:

$$P_{iner} = I\omega/T, \quad (34)$$

where I is the moment of inertia of the wings. A wing's moment of inertia is:

$$I = \int_{l=0}^{l=l_w} M_w' l^2 dl, \quad (35)$$

where M_w' is the mass of a wing element (including wing virtual mass) at a distance l from the shoulder joint. I estimated the moment of inertia of a wing of *R. ferrumequinum* by strip analysis. I spread the wing out and attached it to a stiff card which I cut into 5 mm wide strips (the strips were perpendicular to the long axis of the wing). These strips were weighed to the nearest milligram. I calculated two data sets using oscillation radii for the downstroke (fully extended wing) and the upstroke (flexed wing). I estimated the percentage reduction in wing span during the upstroke by measuring the distance between the wingtips on each successive image of the bat, as seen from the front.

The virtual mass of each strip was calculated and added to the masses of each strip before I was calculated.

Results

I analyzed six flights in detail and a summary of these data is in Table 2. The details of one flight are illustrated in Figs 5–10 and the description that follows is of this flight.

Fig. 5 shows clearly that the animal 'zig-zags' its way up the flight tunnel. Its body is maintained at a tilt angle of approximately 30° and its stroke plane angle is relatively low at about 46° (Fig. 6; Table 2). The resultant force generated by the wings is likely to reach a maximum when the wings are moving fastest, i.e. during the middle third of the downstroke (Fig. 7). We would expect, therefore, that the animal's maximum vertical and horizontal accelerations would occur simultaneously with each other and with maximum wing velocity. However, because of

Table 2. *Kinematics of vertical flight in* Rhinolophus ferrumequinum *(N=6)*

Variable	Abbreviation	Mean	S.D.
Vertical speed	V ($m s^{-1}$)	1.64	0.26
Wingbeat frequency	n (Hz)	10.64	1.19
Positive elevation	θ_u (degrees)	45.90	6.93
Negative elevation	θ_d (degrees)	6.30	12.90
Wingbeat amplitude	θ (degrees)	104.40	16.60
Strokeplane angle	β (degrees)	45.81	9.65
Angle of tilt	α (degrees)	31.07	8.42
Downstroke ratio	τ	0.45	0.03
Downstroke duration	T_d (s)	0.05	–
Upstroke duration	T_u (s)	0.06	0.01

body inertia, these maximum accelerations occur half and one-quarter of a cycle, respectively, *after* the wings have reached their maximum downstroke velocity (Figs 7 and 8).

During the downstroke, the wings generate weight support and thrust. Towards the end of the downstroke, however, negative thrust is produced (Fig. 9). As a result, the animal accelerates, initially forwards and upwards, but then backwards and upwards (Fig. 8). At the beginning of the upstroke, the wings are generating negative thrust and negative weight support (Fig. 9). As the upstroke proceeds, the 'arm' wings are flexed (thus reducing wing span by an average of 65.5 %), but the chiropatagia are accelerated backwards and upwards (relative to the animal) and thrust is therefore generated (Fig. 9). It is clear from Fig. 9 that little or no weight support is generated during the upstroke, although the animal's deceleration exceeds that which would have been expected if the wings were generating no vertical force, indicating that the wings are generating 'negative' weight support (Fig. 8). Towards the end of the upstroke, the animal rapidly extends its wings in preparation for the subsequent downstroke (the 'flick'). This movement also generates thrust.

The most important power component is induced power, net profile, parasite and inertial powers being, respectively, 0.9 %, 1.7 % and 0.2 % of net P_i (0.2564W; Table 3). The total mechanical power of the complete wingstroke is 0.2645W, i.e. 11.92 $W kg^{-1}$, of which 84 % is required during the downstroke.

It is clear from Fig. 10 that muscle power output does not remain constant

Table 3. *Power requirements of vertical flight in* Rhinolophus ferrumequinum *(N=1)*

Induced power, P_i ($W kg^{-1}$)	11.55
Profile power, P_{pro} ($W kg^{-1}$)	0.11
Parasite power, P_{par} ($W kg^{-1}$)	0.20
Inertial power, P_{iner} ($W kg^{-1}$)	0.06
Total power, P_a ($W kg^{-1}$)	11.92

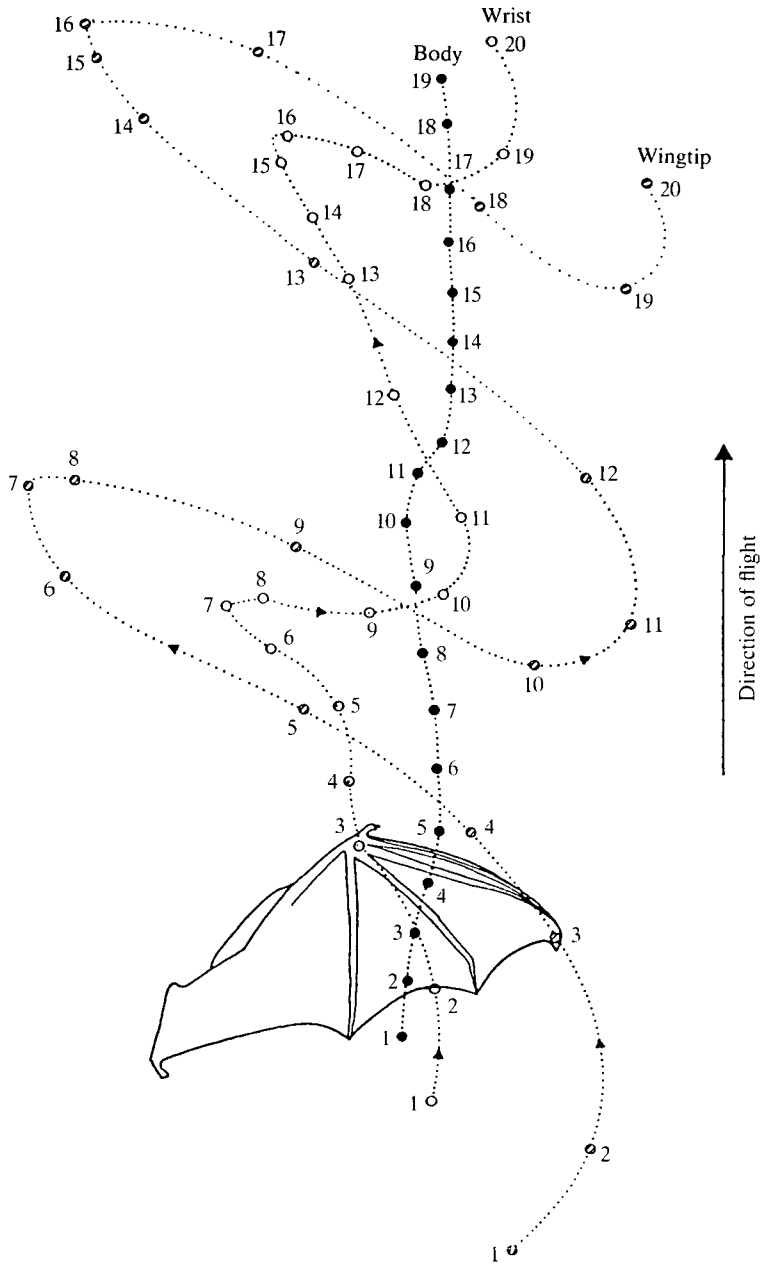

Fig. 5. Tracings of the wing and body movements of *Rhinolophus ferrumequinum* flying vertically up a flight tunnel at an average vertical velocity of 1.64 m s^{-1}. The dots are at 0.01 s intervals. The dots are numbered to show the simultaneous positions of the body (●), wrist (○) and wingtip (⊘).

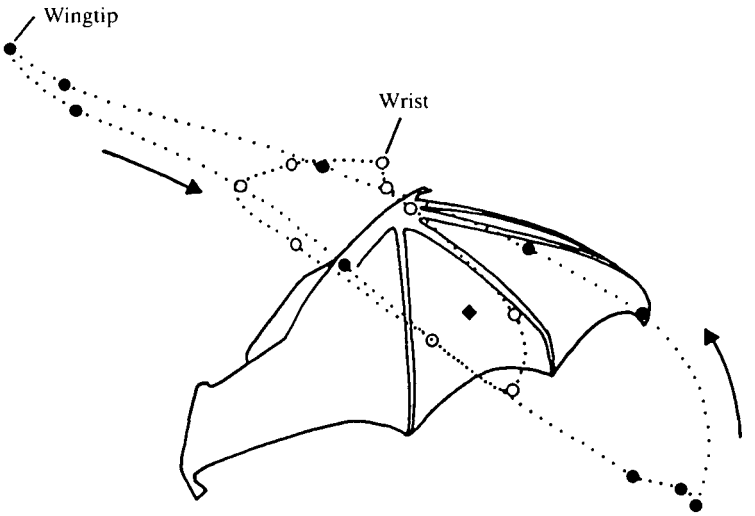

Fig. 6. Lateral projection of the same wingstroke as in Fig. 5, but with tracks traced relative to the bat's nose-leaf. (●) Wingtip; (○) wrist.

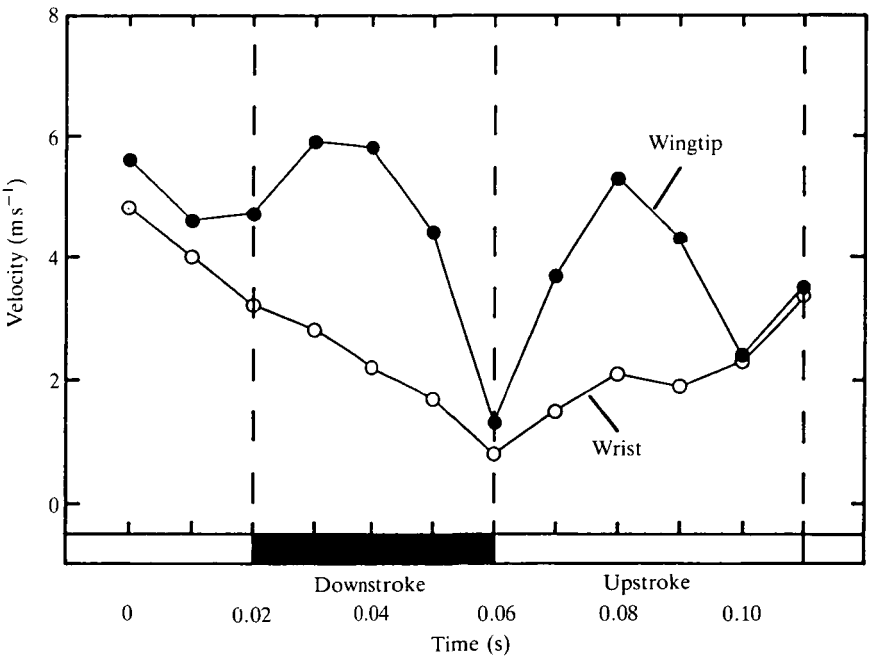

Fig. 7. Wrist (○) and wingtip (●) resultant velocity (i.e. the resultant of V_f, the wing's flapping velocity, and V, the resultant velocity of the body) changes during a wingbeat.

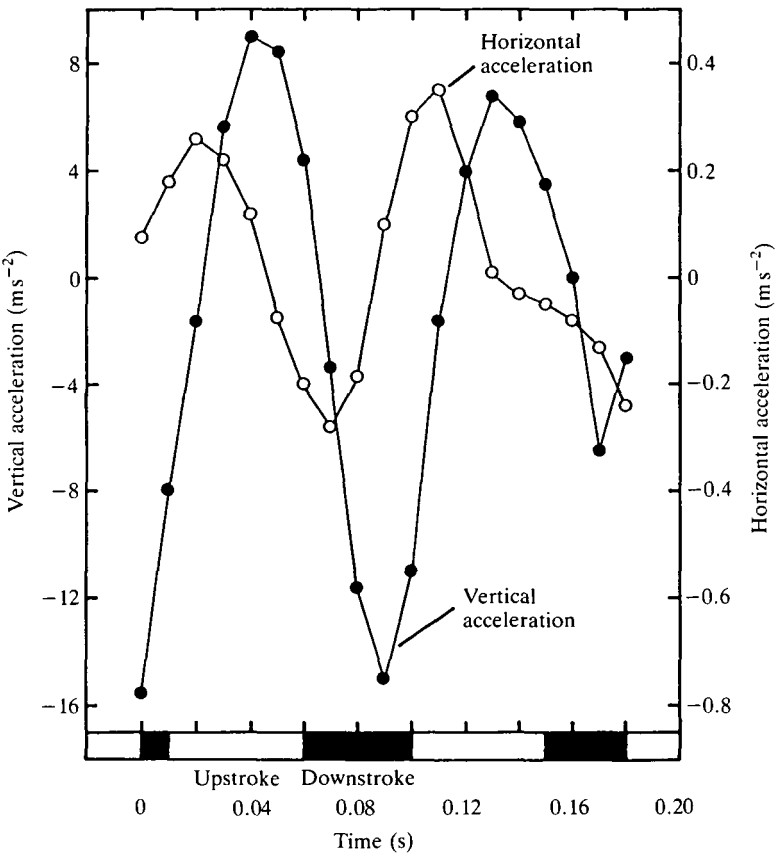

Fig. 8. The vertical (●) and horizontal (○) accelerations of *Rhinolophus ferrum-equinum* flying vertically up a flight tunnel. Two wingbeats are shown.

throughout the wingbeat. At the beginning of the downstroke, power output is low, as the wings are supinated and no aerodynamic work is done. It increases as the downstroke proceeds and the wings are accelerated downwards and forwards. Power output reaches a maximum as the wings attain their maximum downstroke velocity. During the second half of the downstroke, the wings decelerate and power output falls, reaching a minimum at the beginning of the upstroke. Power output rises again during the upstroke, as the wings are accelerated backwards and upwards and thrust is generated. Towards the end of the upstroke, power output falls (as the wings decelerate), only to increase again as the wings are flicked backwards in preparation for the subsequent downstroke.

Discussion

When flying horizontally, animals flap their wings in order to generate thrust while maintaining weight support, and they ensure net positive thrust by altering the wing configuration during the upstroke (Rayner, 1986). At low speeds, bats

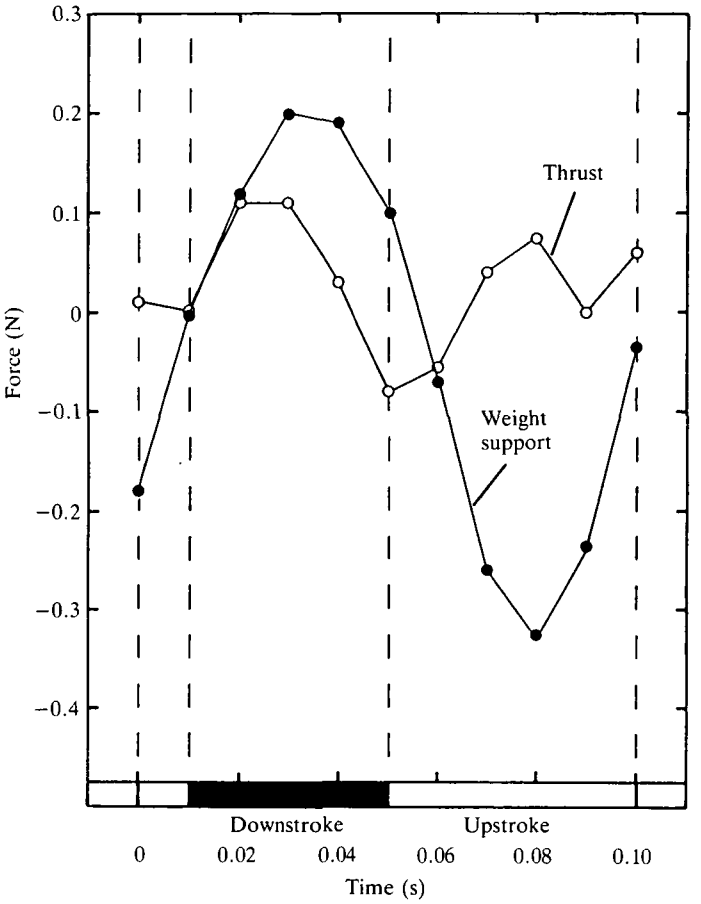

Fig. 9. Curves showing the vertical (●) and horizontal (○) components of the resultant force.

use a 'tip-reversal' upstroke during which the chiropatagia are accelerated backwards and upwards, thereby generating thrust (Eisentraut, 1936; Norberg, 1976*a*; Altenbach, 1979; Aldridge, 1986, 1987*a*). Hovering bats also use the 'tip-reversal' upstroke (Norberg, 1970, 1976*b*; von Helversen, 1986), and the results of this study suggest that the wings are active during this phase of the hovering wingbeat. During the downstroke, weight support and negative thrust are generated, while during the upstroke, the wings generate thrust. In the Introduction I described two possible mechanisms by which the wings could generate thrust during the 'tip-reversal' upstroke (Fig. 1). In the first, the chiropatagia are moved upwards and backwards, with the resultant airflow striking their dorsal surfaces and in this manner generating lift. This lift is directed forwards and therefore acts as thrust. In the second mechanism, the wings are 'flicked' rapidly backwards so that the resultant airflow strikes the dorsal surfaces of the chiropatagia at high incidence angles. Lift is not generated, but the resultant drag acts as thrust. I

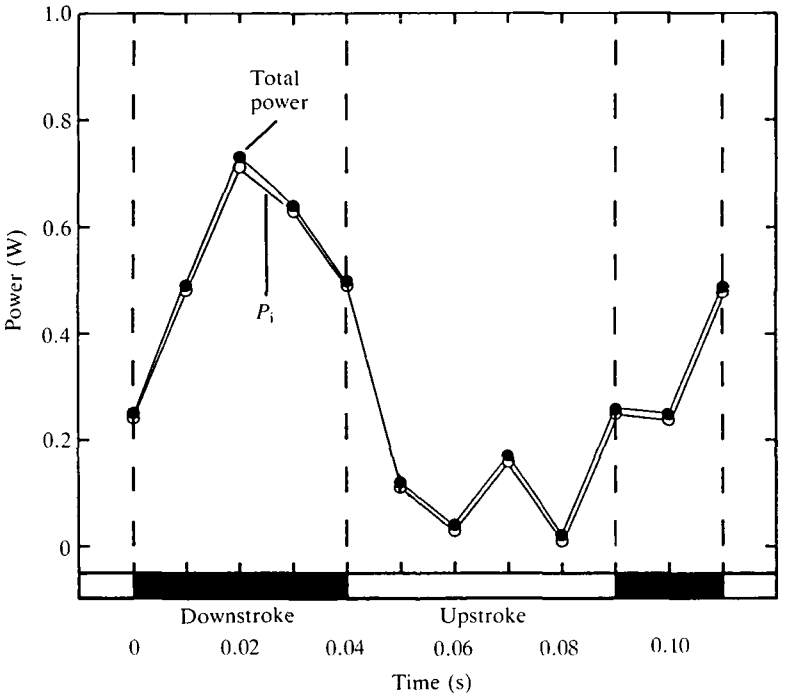

Fig. 10. Changes in mechanical power during the wingbeat. The open circles represent changes in induced power (P_i), whereas the solid circles represent changes in total mechanical power.

would suggest that when flying vertically *R. ferrumequinum* uses both mechanisms to generate thrust during the upstroke. The results indicate that at the beginning of the upstroke no thrust is generated but, as the wings are accelerated backwards, thrust increases and reaches a maximum just after the middle of the upstroke. It then falls, but rises again as the wings are rapidly extended in preparation for the subsequent downstroke. During the first phase the wings may generate lift, while during the flick no lift is generated, but drag acts as thrust.

I have argued in this paper that the vertical flight of *R. ferrumequinum* is equivalent to hovering flight. It is clear that the kinematics of both flight styles are similar; in both *R. ferrumequinum*, climbing vertically, and *P. auritus*, whilst hovering (Norberg, 1970, 1976*b*), wingbeat amplitude is between 100° and 120° and the angle of the body to the horizontal is about 30°. There are differences in wingbeat frequency (between 9 and 11 Hz in *R. ferrumequinum* and between 11 and 12 Hz in *P. auritus*), but these can be explained by the differences in the size of the two species, maximum wingbeat frequency being inversely proportional to $M^{1/3}$ (Pennycuick, 1975). Strokeplane angle in the two species differs by about 15–20°, a difference that cannot be explained as a result of differences in size. The higher strokeplane angles observed in *R. ferrumequinum* result in this species experiencing larger horizontal forces throughout the wingbeat, although net thrust

is zero. Ideally, a hovering animal should only generate vertical forces; it is therefore clear that *R. ferrumequinum* is not hovering 'ideally'. It is possible that *P. auritus* is able to rotate its wings at the humeral joint through a greater angle than is *R. ferrumequinum*, thus enabling this species to have a smaller strokeplane angle and therefore ensuring smaller horizontal forces. This could explain why Norberg (1976*b*) found that upstroke thrust in hovering *P. auritus* was very slight.

As described above, the wingstroke can be divided into three functionally distinct phases: the downstroke, the upstroke and the flick. These phases are powered by different muscle groups and, therefore, it is appropriate for power output to be considered separately for each phase. The downstroke is primarily powered by Mm. pectoralis, serratus anterior, subscapularis, clavodeltoides and latissimus dorsi (Hermanson and Altenbach, 1983), which are required to generate approximately 84 % of total mechanical power, i.e. $10.01\,W\,kg^{-1}$. In the past it has been assumed that the upstroke in hovering flight is essentially a recovery stroke and, therefore, that the muscles that power it are only required to work against wing inertia, i.e. in this example, to generate about $1.33\times10^{-3}\,W\,kg^{-1}$. However, the results of this study make it clear that the animal's wings are active during the upstroke, generating thrust. Hermanson and Altenbach (1983) have shown that the abductor muscles (Mm. spinodeltoideus, acromiodeltoideus, the trapezius group and M. triceps brachii) are active throughout the upstroke, but that towards the end the adductors become active and are probably responsible for powering the flick. If this is the case in *R. ferrumequinum*, the abductor muscles are responsible for approximately 50 % of the total mechanical power during the upstroke (i.e. $0.69\,W\,kg^{-1}$). During the flick, the adductor muscles generate approximately $0.69\,W\,kg^{-1}$. Overall, the adductor muscles are responsible for generating about 90 % of the power required for vertical flight in *R. ferrumequinum*.

It is interesting to compare the power required by *R. ferrumequinum* for vertical flight with the power required by this species for other characteristic flight behaviours. The relationship between power and flight speed for a particular individual can be defined by the required powers for three flight behaviours: (1) stationary hovering flight, P_{ih}, (2) horizontal flight at the speed at which required power is at a minimum (minimum power speed, V_{mp}), P_{am}, and (3) horizontal flight at the speed at which the power/speed ratio reaches a minimum (i.e. maximum range speed, V_{mr}), P_{mr}. For the individual *R. ferrumequinum* used in this study P_{ih}, P_{am} and P_{mr} are, respectively, $11.02\,W\,kg^{-1}$, $4.72\,W\,kg^{-1}$ ($V_{mp}=4.84\,m\,s^{-1}$) and $5.39\,W\,kg^{-1}$ ($V_{mr}=6.39\,m\,s^{-1}$). Vertical flight therefore requires 8 %, 150 % and 120 % more power than is required for stationary hovering flight and flight at V_{mp} and V_{mr}, respectively.

Finally, it is necessary to consider how reliable is my estimate of the power required for vertical flight in *R. ferrumequinum*. When compared with estimates of the power required by *R. ferrumequinum* for level flight using Pennycuick's (1989) and Rayner's (Norberg and Rayner, 1987) models, my estimate seems reasonable, being approximately 50 % higher than both. However, Norberg (1976*a*) estimated

that the metabolic flight cost for level flight in a 0.009 kg *P. auritus* was approximately 17 times basal metabolic rate (BMR). For a 0.0222 kg *R. ferrumequinum* in level flight, this would mean a metabolic flight cost of approximately 165 W kg^{-1} [using Stahl's (1967) equation for resting metabolic rate to estimate BMR]. The comparable value for a vertically flying *R. ferrumequinum* is approximately 60 W kg^{-1} (calculated using the estimate of mechanical power given above), i.e. at least 60 % lower than one would have expected. Similarly this value is significantly lower than equivalent estimates for level flight calculated from respiratory and doubly labelled water data (Racey and Speakman, 1987; Norberg, 1990), which, like Norberg's estimates (1976*a*), suggest that flight costs are approximately 15–20 times BMR.

There are no clear reasons for these discrepancies, although a number of suggestions can be made. For example, to estimate metabolic flight costs for vertical flight I assumed that mechanical efficiency (i.e. the efficiency by which chemical power is converted into mechanical power) was 0.20. Measured values of mechanical efficiency in bats can be as low as 0.12 (Thomas, 1975), a value that would almost double my estimate of metabolic flight costs for vertical flight. Similarly, the physiological methods may overestimate flight costs (e.g. Tucker, 1972).

Clearly, we need to know a great deal more about the mechanism by which flying animals convert chemical power into mechanical power before we will be able to explain the discrepancies in the results obtained by different techniques.

List of symbols

a_b	Acceleration of the body due to wing inertia
a_w	Acceleration of the centre of mass of a wing
a_z	Vertical acceleration of the body
a_x	Horizontal acceleration of the body
A_e	Equivalent flat-plate area
b	Wing span
c	Wing chord
$C_{d,par}$	Parasite drag coefficient
$C_{d,pro}$	Profile drag coefficient
d_d	Distance, within the strokeplane, between the wrist and the longitudinal axis of the body at the end of the downstroke
d_u	Distance, within the strokeplane, between the wrist and the longitudinal axis of the body at the beginning of the downstroke
D_i	Induced drag
D_{par}	Parasite drag
D_{pro}	Profile drag
F	Resultant force acting on the bat
F_b	Inertial forces on the animal due to wing oscillation

F_w	Total inertial force acting on the body due to the acceleration of one wing
g	Acceleration due to gravity
I	Wing moment of inertia
k	Induced power factor
l	Distance of a wing element from the humeral joint
l_p	Distance between a point midway between the two humeral joints and the wrist when the wing is fully extended
l_w	Wing length
L	Lift
m_v	Wing virtual mass
m_v'	Virtual mass of a wing element
M	Body mass
M_w	Wing mass
M_w'	Mass of a wing element
n	Wingbeat frequency
P_a	Total mechanical power
P_{am}	Minimum power
P_i	Induced power
P_{ih}	Induced power of hovering
P_{iner}	Inertial power
P_{mr}	Maximum range speed power
P_{par}	Parasite power
P_{pro}	Profile power
Q_s	Wing loading
r	Distance between the centres of mass of the wing and body
R	Aspect ratio
S	Wing area
S_b	Projected area of the body perpendicular to the airflow
S_d	Wing disk area
T	Wingbeat duration
T_d	Downstroke duration
T_u	Upstroke duration
V	Resultant velocity of the body
V_{mp}	Minimum power speed
V_{mr}	Maximum range speed
V_f	Flapping velocity of the wing
V_i	Induced velocity
V_R	Resultant velocity of the wing
α	Angle of body to the horizontal
β	Strokeplane angle
τ	Downstroke ratio
θ	Amplitude
θ_u	Positive elevation of the wing

θ_d Negative elevation of the wing
ϕ Positional angle
ρ Air density
ω Angular velocity
$\dot{\omega}$ Angular acceleration

This research was funded by the Natural Environment Research Council and the Science and Engineering Research Council. I am grateful to Drs C. J. Pennycuick, J. M. V. Rayner, K. D. Scholey, S. Dow and S. S. Burtles for their assistance and support during the course of the work. Drs U. M. Norberg, Å. Norberg and J. W. Hermanson read an earlier version of the manuscript and I am grateful for their comments.

References

ALDRIDGE, H. D. J. N. (1986). Kinematics and aerodynamics of the greater horseshoe bat, *Rhinolophus ferrumequinum*, in horizontal flight at various speeds. *J. exp. Biol.* **126**, 479–497.

ALDRIDGE, H. D. J. N. (1987*a*). Body accelerations during the wingbeat in six bat species: the function of the upstroke in thrust generation. *J. exp. Biol.* **130**, 275–293.

ALDRIDGE, H. D. J. N. (1987*b*). Turning flight of bats. *J. exp. Biol.* **128**, 419–425.

ALDRIDGE, H. D. J. N. (1988). Flight kinematics and energetics in the little brown bat, *Myotis lucifugus* (Chiroptera: Vespertilionidae), with reference to the influence of ground effect. *J. Zool., Lond.* **216**, 507–517.

ALDRIDGE, H. D. J. N., OBRIST, M., MERRIAM, H. G. & FENTON, M. B. (1990). Roosting, vocalisations and foraging by the African bat, *Nycteris thebaica*. *J. Mammal.* **71**, 242–246.

ALTENBACH, J. S. (1979). Locomotor morphology of the vampire bat, *Desmodus rotundus*. *Spec. Publs Am. Soc. Mammal.* **6**, 1–75.

BROWN, R. H. J. (1948). The flight of birds. *J. exp. Biol.* **25**, 322–333.

EISENTRAUT, M. (1936). Beitrag zur Mechanik des Fledermausfluges. *Z. wiss. Zool.* **24**, 95–104.

ELLINGTON, C. P. (1984). The aerodynamics of hovering insect flight I–VI. *Phil. Trans. R. Soc. Ser.* B **305**, 1–181.

HERMANSON, J. W. AND ALTENBACH, J. S. (1983). The functional anatomy of the shoulder of the pallid bat, *Antrozous pallidus*. *J. Mammal.* **64**, 62–75.

LANCZOS, C. (1957). *Applied Analysis*. London: Isaac Pitman & Sons.

NORBERG, U. M. (1970). Hovering flight of *Plecotus auritus* Linneaus. *Bijr. Dierk.* **45**, 62–66.

NORBERG, U. M. (1976*a*). Aerodynamics, kinematics and energetics of horizontal flight in the long-eared bat *Plecotus auritus*. *J. exp. Biol.* **65**, 179–212.

NORBERG, U. M. (1976*b*). Aerodynamics of hovering flight in the long-eared bat *Plecotus auritus*. *J. exp. Biol.* **65**, 459–470.

NORBERG, U. M. (1990). *Vertebrate Flight*. Berlin: Springer-Verlag.

NORBERG, U. M. AND RAYNER, J. M. V. (1987). Ecological morphology and flight in bats (Mammalia; Chiroptera): wing adaptations, flight performance, foraging strategy and echolocation. *Phil. Trans. R. Soc. Ser.* B **316**, 335–427.

PENNYCUICK, C. J. (1967). The strength of the pigeon's wing bones in relation to their function. *J. exp. Biol.* **46**, 219–233.

PENNYCUICK, C. J. (1975). Mechanics of flight. In *Avian Biology*, vol. 5 (ed. D. S. Farner, J. R. King and K. C. Parkes), pp. 1–73. London: Academic Press.

PENNYCUICK, C. J. (1989). *Bird Flight Performance: A Practical Calculation Manual*. Oxford: Oxford University Press.

PENNYCUICK, C. J., OBRECHT, H. H., III AND FULLER, M. R. (1988). Empirical estimates of body drag in large waterfowl and raptors. *J. exp. Biol.* **135**, 253–264.

RACEY, P. A. AND SPEAKMAN, J. R. (1987). The energy costs of pregnancy and lactation in heterothermic bats. *Symp. zool. Soc. Lond.* **57**, 107–125.

RAYNER, J. M. V. (1979). A new approach to animal flight mechanics. *J. exp. Biol.* **49**, 527–555.

RAYNER, J. M. V. (1986). Vertebrate flapping flight mechanics and aerodynamics and the evolution of flight in bats. In *Biona Report*, vol. 5, *Fledermausflug* (ed. W. Nachtigall). Heidelberg: Gustav Fischer-Verlag.

RAYNER, J. M. V. AND ALDRIDGE, H. D. J. N. (1985). Three-dimensional reconstruction of animal flight paths and the turning flight of microchiropteran bat. *J. exp. Biol.* **118**, 247–265.

RAYNER, J. M. V., JONES, G. AND THOMAS, A. (1986). Vortex flow visualisations reveal change in upstroke function with flight speed in bats. *Nature* **321**, 113–114.

STAHL, W. R. (1967). Scaling of respiratory variables in mammals. *J. appl. Physiol.* **22**, 453–460.

THOMAS, S. P. (1975). Metabolism during flight in two species of bats, *Phyllostomus hastatus* and *Pteropus gouldii*. *J. exp. Biol.* **63**, 273–293.

TUCKER, V. A. (1972). Metabolism during flight in the laughing gull, *Larus atricilla*. *Am. J. Physiol.* **222**, 237–245.

TUCKER, V. A. (1973). Bird metabolism during flight: Evaluation of a theory. *J. exp. Biol.* **58**, 689–709.

VON HELVERSEN, O. (1986). Blutenbesuch bei Blumenfledermausen: Kinematik des Schwirrfluges und Energiebudget im Freiland. In *Biona Report*, vol. 5, *Fledermausflug* (ed. W. Nachtigall). Heidelberg: Gustav Fischer-Verlag.